Arabian Journal of Chemistry (2014) 7, 1039–1048

King Saud University

Arabian Journal of Chemistry

www.ksu.edu.sa
www.sciencedirect.com

ORIGINAL ARTICLE

Molecular interactions of CPC, CPB, CTAB, and EPC biosurfactants in aqueous olive oil mixtures analyzed with physicochemical data and SEM micrographs

Man Singh [a,b,*], Neeti Chaudhary [a], R.K. Kale [c], H.S. Verma [d]

[a] *Chemistry Research Lab., Deshbandhu College, University of Delhi, New Delhi 110 019, India*
[b] *School of Chemical Sciences, Central University of Gujarat, Gandhinagar, India*
[c] *School of Life Science, Jawaharlal Nehru University, New Delhi 110 067, India*
[d] *Department of Chemistry, J.V. College, Baraut, CCS University, Meerut, India*

Received 2 February 2010; accepted 30 December 2010
Available online 18 January 2011

KEYWORDS

Survismeter;
SEM;
Biosurfactants;
Olive oil;
Interactions

Abstract Structural studies of olive oil–water–biosurfactants mixtures are most attracting for several academic as well as industrial significances. Thus, densities (ρ), viscosities (η), and surface tensions (γ) of cetylpyridinium chloride (CPC) and bromide (CPB), cetyltrimethylammonium bromide (CTAB) and egg-phosphatidylcholine (EPC) biosurfactants (BS) 2–10 mm kg^{-1} in olive oil + water mixture in 2 mm kg^{-1} interval at 310.15 K are reported. The densities were for apparent molal volume (V_ϕ/10^{-6} m^3 mol^{-1}), η and γ determinations. The viscosities were fitted in extended Jones–Doles equation for intrinsic viscosity (B, kg mol^{-1}) and slope (D, kg mol^{-1})^2 derivation. The γ and V_ϕ data were regressed for their limiting γ^0 and V_ϕ^0 data and the SEMs were illustrated surface morphology. The EPC caused maximum oil–water dissolution as compared to other surfactants. Intramolecular multiple force theory [IMMFT] is proposed to explain molecular interactions of olive oil–water–EPC mixtures with a possible correlation of surface and bulk reorientations with

* Corresponding author at: Chemistry Research Lab., Deshbandhu College, University of Delhi, New Delhi 110 019, India.
E-mail addresses: mansingh50@hotmail.com (M. Singh), neeti.chaudhry@gmail.com (N. Chaudhary), raosahekale@gmail.com (R.K. Kale).

Peer review under responsibility of King Saud University.

Production and hosting by Elsevier

http://dx.doi.org/10.1016/j.arabjc.2010.12.034

microstructures depicted with SEM. Frictional and cohesive forces as Friccohesity have been noted as driving forces to assert for validity of the IMMFT model and its link with SEM.

1. Introduction

Molecular activities individually and in mixtures are initials and signatures for origin of scientific simulations and frameworks for academic as well as new industrial upcoming. How do the molecules maintain identity in a mixture of different polarity and electrostatics and consequently undergo structural reorientations? It is more important with biomolecules such as EPC which being weakly polar involved in molecular interactions as emulsifying agent (Ponder and Case, 2003; Warshel et al., 2006; Schutz and Warshel, 2001). A detection of bound water molecules at moon is an input and incentive to intensify search and research of undiscovered molecular world (Israelachvili, 1992). In year 1953, Stanley and Miller experiment was a pioneer model to signify molecular signatures. Similarly, several experiments and functions of matter have strengthened a concept of molecular science (Leckband and Israelachvili, 2001) in search of newer mixtures and properties (Koehl and Levitt, 1999). The molecular sciences were studied by many scientists (Brunger and Adams, 2002) for peculiar structural reorientation optimized to facilitate interactions (Edgcomb and Murphy, 2000). Since 17th to 19th centuries, several workers intensified efforts to elucidate hidden molecular combinations in different polarities (Mendes et al., 2002). For example, Van der Waals put up best efforts to establish conducting and transporting properties along binding forces (Rohl et al., 2004). Debye–Huckle theory and Lennard-Jones potential distinguished a basic difference in potential and kinetics of molecular dispersion and motions (Lomize et al., 2006). Theoretically Schrödinger and Born Oppenheimer Approximation (BOA) focused nuclear charge contribution in molecule based on quantum chemistry.

A molecular potential before mixing is zero but on mixing it is not zero due to interactions (Lomize et al., 2002). Oil and water (Murphy and Gill, 1991) are not much soluble due to weaker interactions (Shakhnovich and Finkelstein, 1989) but the BOA conceptually explains their interactions which are extended to simple organic or inorganic molecules/complexes (Graziano et al., 1996). In such situations the forces inside a molecule are confined to a center of control. Onsager and Debye–Huckle, explained a contribution of electrostatics poles of either single ions Na^+, Ca^+, NH_4^+ or Zwitterions like amino acids where alignments of solvents were fitted with molecular electrostatics (Myers and Pace, 1996). The olive oil does not hold any charge so Debye–Huckle equation is not of much use and offered solutions of polar molecules. Debye could not offer adequate solutions to macromolecules even with proteins as partially ionic peptide bonds were embedded in folding and electrostatic poles were not clearly exposed to solvents (Brunger, 2002). So the solvents reorientation was offered to approach embedded electrostatics poles to unfolds the proteins and similar others. Tanford conducted substantial studies on interactions useful for biochemists and biothermodynamists (Guntert, 1998). Ludvig Lorenz further refined such interactions and approaches of molecular forces, especially of weaker electrolytes as surfactants and mildly partial such as olive oil where forces are confined, redistributed in a zonal hobnobbing. This made a better understanding of organic mixtures in a wider way to study oil–water muslins for industrial purposes. For centuries, the molecular framework has been a fascination to scientists for molecular design, polarity, electronic configurations and others. Since origin of life, it has been a never ending process and the scientists, chemists, biochemists, biotechnologists continued their pursuit for further search of either developing new mixtures in laboratories or extracting out of natural sources animal or plants (Shakhnovich and Finkelstein, 1989). Further, Van der Waals, Lennard and others worked on primitive part of molecular sciences and realized a lot more potential and science hidden in mixtures which have been furthered various new scientific theories, options, surfaces, intra-surfaces like nanotechnology. Thermodynamics was tried to retrieve hidden molecular energetics such as entropic and free energy changes (Warshel and Levitt, 1976). The studies of mixtures are continued and molecular scientists remarkably contributed to further elaborate and signify a molecular potential for industrial uses.

From 18th to 19th centuries, a shift from ionic to molecular approaches was noted on a pattern of big debate on existence of atomic theory put forward by Nellie Bohr and with practical evidence, an existence of atomic theory was accepted. Ionic mixtures are easy to explain but oil and water mixtures with additives need classical support in favor of molecular origin of forces responsible for mixtures. Though several intensely diversified conflicts of molecular sciences were noted but a molecular force theory (MFT) was unanimously accepted which is still continued. Since late 20th to 21th century, trends to develop supra or giant molecules in laboratories either based on metallic ions such as transitional and lanthanides metals (Singh and Sushma, 2009) or certain molecular rings as core/centermost part or then after branching as an extension for molecular shape and sizes developed for industrial relevance (Singh et al., 2008). These sciences revolved around MFT, and originated several diversified molecular forces theories (DMFT) to understand vivid molecular fascinations using thermodynamics, chemical kinetics, and electrochemistry which thinly peeped into inner sides of molecular interactions. The DMFT was put forward and new phenomenon such as friccohesity was emerged to find out a relevance of macromolecules to materials science like polymers, textile, dyeing, drugs, cosmetics, sol gel, electrolytes, solvents, coolants, pesticides, disinfectants, so on and so forth.

It aimed to enrich and open new gates of knowledge for industrialization of molecular concept in interest of society. For example, olive oil–water–bio-surfactants mixtures were never designed and studied, despite huge industrial potential (Singh and Sharma, 2006). The mixtures like ours are as parts of daily use, for example, tooth pastes, soaps, detergents, oil painting, proteins, carbohydrates, vitamins, cosmetics, textiles, inks, food, paper pulp, polymers, glass materials and what not are essential commodities. Hence present study is novel approach and fabulous attraction. Fundamentally, molecular interactions involve bond disruption, reorientation, breaking, bond angle and bond energy. These are of industrial values

and need of an hour to further correlate and reveal molecular mechanism. For example, hydrocarbons offer energy to man and vehicles to gear up world on wheels even moving to moon using semisolid silicon carbide as fuels to rocket launchers or aero plane. So society is most benefited with molecular fascination such as electronic display in liquid crystals and hence molecular interactions of CPC, CPB, CTAB, and EPC as biosurfactants were chosen. An intramolecular multiple force theory (IMMFT) is a model and it was proposed to intuitively explain the interactions. The IMMFT could excellently interpret surface as well as bulk dynamics responsible for microstructure illustrated with SEM micrographs. The IMMFT is a step forward in molecular approaches of the science and technology. Around phosphate atom of EPC, three different alkyl chains with O atoms are fitted which cause different force centers within an EPC molecule. It favors diffused hydrophilic interactions especially useful for emulsification or homogenous dispersion in bulk water phase and not moves to surface contrary to CTAB, CPC, and CPB which accumulate at surface (Singh and Kumar, 2006). Thus two different interaction activities take place with them as EPC prefers to be in bulk phase but the CTAB, CPC, and CPB move to surface and strongly weaken tension. Hence the IMMFT explained the maximum dissolution with EPC.

2. Experimental

The CPC and CPB (AR, 99.99% CDH, Bombay, India), CTAB (AR, 99.99% GS Chemical Testing Lab & allied industries, Bombay, India) and L-α-phosphatidylcholine from egg yolk (AR, Fluka, USA) were used as received. Olive oil was distilled as per standard methods. Millipore water was used for solutions, w/w, with ± 0.01 mg precision on Dhona balance (Singh and Kumar, 2006) with $\pm 10^{-5}$ mol kg^{-1} uncertainties. The 2–10 mm kg^{-1} BS mixtures in 2 mm kg^{-1} interval were studied. The 1:1000 olive oil with water stock solution was used for measurements. Densities were obtained with bicapillary pyknometer, using electronic balance, 0.01 mg Dhona, model 100 DS, a procedural details are reported elsewhere (Singh, 2006). The densities were reproducible to $\pm 10^{-2}$ kg m^{-3} with ± 0.01 °C temperature control, checked with Beckmann thermometer. Prior to measurements, the mixtures were equilibrated for 20 min in a thermostatically controlled water bath. Flow times and pendant drop counts were measured with Survismeter with 10^{-2} s electronic timer and electronic counter, respectively. An air filter was used for high quality air for pressure gradient inside functional bulbs of survismeter for lifting up the liquids, the details are reported elsewhere (Singh, 2009). Since the chosen mixtures were of biophysical significance hence no suspended particulate matter (SPM), moisture, and contaminated air were permitted to touch the samples during measurements. The SEMs were recorded with scanning electron microscope model LEO 435 VP from Electron Microscope Facility, AIIMS, New Delhi, under sterilized condition.

3. Results and discussion

Densities were calculated with Eq. (1).

$$\rho = \left(\frac{w - w_e}{w_0 - w_e}\right)\rho_0 + 0.0012\left(1 - \left(\frac{w - w_e}{w_0 - w_e}\right)\right) \quad (1)$$

The ρ solution, ρ^0 solvent and 1.2 kg m^{-3} air densities, respectively, the $(1 - (w - w_e)/(w_0 - w_e))$ is a buoyancy correction for air. The w_e, w_0, and w are weights of empty, solvent, and solution filled pyknometer, respectively. Errors were statistically evaluated. The viscosities were calculated with Eq. (2).

$$\eta = \left(\frac{\rho t}{\rho_0 t_0}\right)\eta_0 \quad (2)$$

The t and t_0 flow times and η and η_0 are viscosities of solution and solvent respectively, relative viscosities ($\eta_{rel} = \eta/\eta_0$) and errors were analyzed as usual. The η_{rel} data were calculated with extended Jones–Dole equation given below.

$$\eta_{rel} = \frac{\eta}{\eta_0} = B + Dc + Dc^2 \quad (3)$$

The c *is* concentration, B *is* viscosity constant, and D is slope. The surface tension was calculated with Eq. (4).

$$\gamma = \left(\left(\frac{n_0}{n}\right)\left(\frac{\rho}{\rho_0}\right)\right)\gamma_0 \quad (4)$$

The n pendant drop numbers for solution and n_0 for solvent, the γ and γ^0 are surface tensions of solution and solvent, respectively. The V_ϕ was calculated with Eq. (5).

$$V_\phi = \left[\frac{1000(\rho_0 - \rho)}{m\rho\rho_0}\right] + \left(\frac{M}{\rho}\right) \quad (5)$$

The M solute molar mass, m molality, the ρ and ρ^0 are densities of solution and of the water, and error in V_ϕ^0 were

Table 1 Density $(\rho)/10^3$ kg m^{-3}, viscosity $(\eta)/10^{-1}$ kg m^{-1} s^{-1}, surface tension (γ)/mN m^{-1}, apparent molal volume $(V_\phi)/10^{-6}$ m^3 mol^{-1} and reduced viscosity (η_{red})/kg mol^{-1} of CPC, CPB, CTAB, and EPC in olive-oil–water (OOW) mixtures.

Concentration	ρ	η	γ	V_ϕ	η_{red}
CPC + OOW					
0.002	0.99254	0.73269	42.54	763.20	26.2835
0.004	0.99300	0.73515	41.69	449.73	13.989
0.006	0.99343	0.74151	41.70	349.51	10.8729
0.008	0.99270	0.74178	41.67	442.53	8.20217
0.01	0.99280	0.74084	41.68	416.00	6.42737
CPB + OOW					
0.002	0.99273	0.73175	38.53	716.66	25.6064
0.004	0.99335	0.73322	37.15	407.51	13.3314
0.006	0.99359	0.73171	35.86	367.15	8.52589
0.008	0.99377	0.73583	35.24	353.91	7.13416
0.01	0.99334	0.73942	35.23	407.65	6.22306
CTAB + OOW					
0.002	0.99296	0.73125	44.40	563.44	25.24512
0.004	0.99314	0.73347	40.06	421.77	13.42051
0.006	0.99374	0.73540	39.31	304.67	9.408730
0.008	0.99276	0.73299	38.53	440.54	6.624387
0.01	0.99283	0.73398	38.53	419.57	5.441934
EPC + OOW					
0.002	0.99137	0.80634	67.98	1745.00	79.18255
0.004	0.99125	0.83884	65.77	1286.07	51.26445
0.006	0.99122	0.88624	67.96	1117.27	45.52488
0.008	0.99121	0.91964	70.31	1031.43	40.14076
0.01	0.99123	1.02076	70.31	976.83	46.63947

calculated with $V_\phi = \pm\Delta\,\rho 1000\,\mathrm{m}^{-1}$ relation. The V_ϕ data were fitted in equation given below.

$$V_\phi = V_\phi^0 + S_V m^{1/2} + S_v' m \quad (6)$$

The V_ϕ^0 limiting apparent molal volume and S_v and S_v' are 1st and 2nd degree slopes respectively. The ρ, η, γ, V_ϕ, and η_{red} data of BS with olive-oil–water (OOW) are noted in Table 1 and regression constants in Table 2. The $\rho^0/10^3\,\mathrm{kg\,m^{-3}}$ of BS and slopes $S_d/10^3\,\mathrm{kg^2\,m^{-3}\,mol^{-1}}$ are depicted in Fig. 1 and reduced viscosity $(\eta_{red})/\mathrm{kg\,mol^{-1}}$ with $\mathrm{mol\,kg^{-1}}$ in Fig. 2. A comparison of surface tensions of BS is shown in Fig. 3, the V_ϕ data in Fig. 4 and the SEMs in Fig. 5 along molecular structures in Fig. 6.

3.1. Densities

Limiting density ρ^0 is a function of interacting strength of solute and the ρ^0 data of the surfactants with olive oil + water mixture are as CTAB > CPC > CPB > EPC (Table 1). The higher values of the CTAB inferred stronger molecular interactions and the lower of the EPC the weaker than those of the CPC and CPB. The CPC and CPB had similar cetyl chains and pyridine ring with the Cl^- and Br^- anions, respectively. The ionic effect of smaller sized Cl^- with the CPC produced higher ρ^0 than those of the CPB. The CPC and CPB with pyridine rings caused stronger intermolecular force (IMF) due to π-conjugation. The CTAB without pyridine ring and with a quaternary nitrogen atom (N^+) and cetyl chain alike CPC and CPB produced the higher ρ^0 values than those of the CPC and CPB. Hence the activities of π-conjugation in hydrophobic–hydrophilic interactions where the surfactants have multiple centers of forces such as hydrophobic forces along alkyl chain and hydrophilic forces along hydrophilic parts. The water interacts differently with these configurations of the surfactants. Similarly, the EPC with an N^+ atom alike CPC, CPB, and CTAB and additional PO_4^{-3} and 2 cetyl chains (Fig. 6) produced lowest ρ^0 data with almost two times higher hydrophobic interactions than of other the BS. The EPC with different molecular configuration interacted differently due to intramolecular multiple forces [IMMF] and model is noted as intramolecular multiple forces theory [IMMFT]. Since the EPC is centered on phosphate P atom with three alkyl chains which surround the P (Fig. 6). The molecule has steric and induction effects with covalent bonding force (CBF) which with double bond with each alkyl chains with sp^2 configuration that conceptually weakened the CBF. Each alkyl chains attached with O atoms with different electronic configuration and CBF. With EPC different force centers with single molecule are operational and caused different activities because of that the EPC molecule caused effects weaker on surface activities. Similarly the olive oil with different force centers induced different alignments such as benzene ring with π-conjugation center developed a shifting charge centers. Also alkyl chains broken with O_2 caused different forces within single molecule and a double within terminal chain also caused many operational forces centers. The IIMFT theory offers a better solution to structurally explain molecular forces responsible for emulsification action of the EPC as it has not largely reduced the surface tension and does not tend toward interface. The IMMFT is valid as the EPC molecule does not behave like CPC, CPB, CTAB where their alkyl chain caused hydrophobic

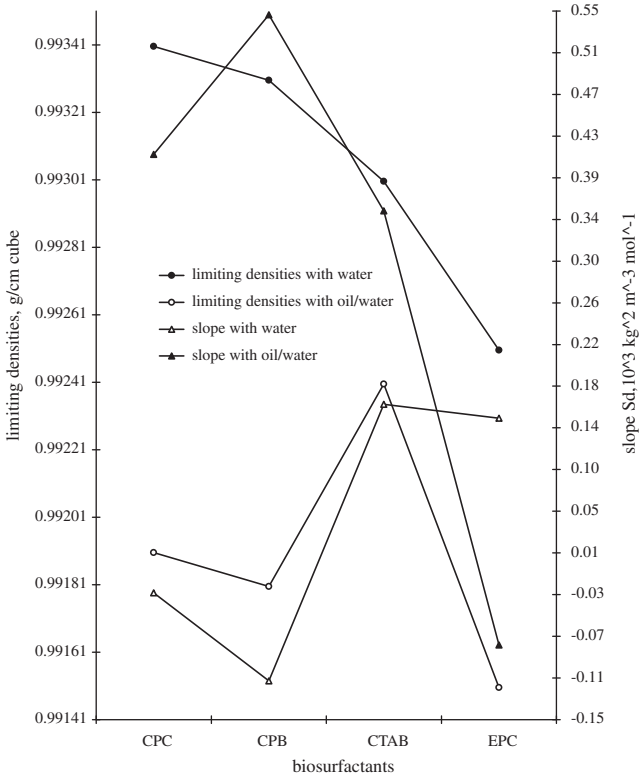

Figure 1 Limiting densities $\rho^0/10^3\,\mathrm{kg\,m^{-3}}$ of BS with water > oil/water and slopes $S_d/10^3\,\mathrm{kg^2\,m^{-3}\,mol^{-1}}$.

Table 2 The $\rho^0/10^3\,\mathrm{kg\,m^{-3}}$, $V_\phi^0/10^{-6}\,\mathrm{m^3\,mol^{-1}}$, η^0, i.e., $B/\mathrm{kg\,mol^{-1}}$ and $\gamma^0/\mathrm{mN\,m^{-1}}$ are limiting functions and $S_d/10^3\,\mathrm{kg^2\,m^{-3}\,mol^{-1}}$, $S_v/10^{-6}\,\mathrm{kg\,m^3\,mol^{-1}}$ and $S_v'/10^{-6}\,\mathrm{kg^2\,m^3\,mol^{-3}}$, JD/$\mathrm{kg^2\,mol^{-2}}$ and $S\gamma^0/\mathrm{mN^{-1}\,kg\,mol^{-1}}$ are slopes of density, apparent molal volume, viscosity, and surface tension, respectively.

ρ^0	S_d	V_ϕ^0	S_v	S_v'	B	JD	γ^0	$S\gamma^0$
CPC + OOW								
0.9919	0.4094	1078.2	−199461	1.00E + 07	37.55	−6878.8	43.2	−441.64
CPB + OOW								
0.9918	0.5485	983.69	−194890	1.00E + 07	38.72	−7850	40.66	−1155.5
CTAB + OOW								
0.9924	0.3532	751.38	−119386	9.00E + 06	37.21	−7144.1	48.48	−2519.9
EPC + OOW								
0.9915	−0.079	1808.9	−280644	2.00E + 07	110.01	−18637	67.98	−516.28

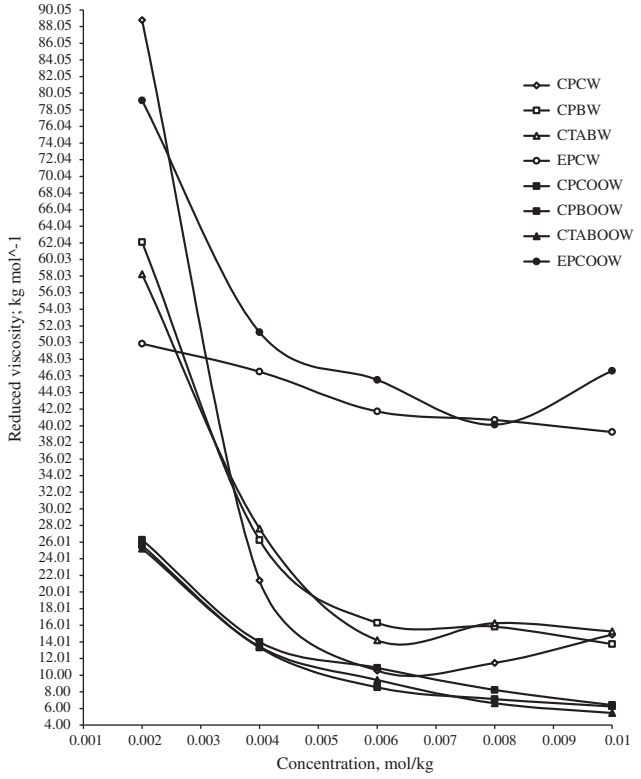

Figure 2 Comparative decrease in reduced viscosity (η_{red})/kg mol^{-1} with concentration (mol kg^{-1}) of CPC, CPB, CTAB, and EPC from 0.002 to 0.01 mol kg^{-1} with water (W) and olive-oil/water (OOW).

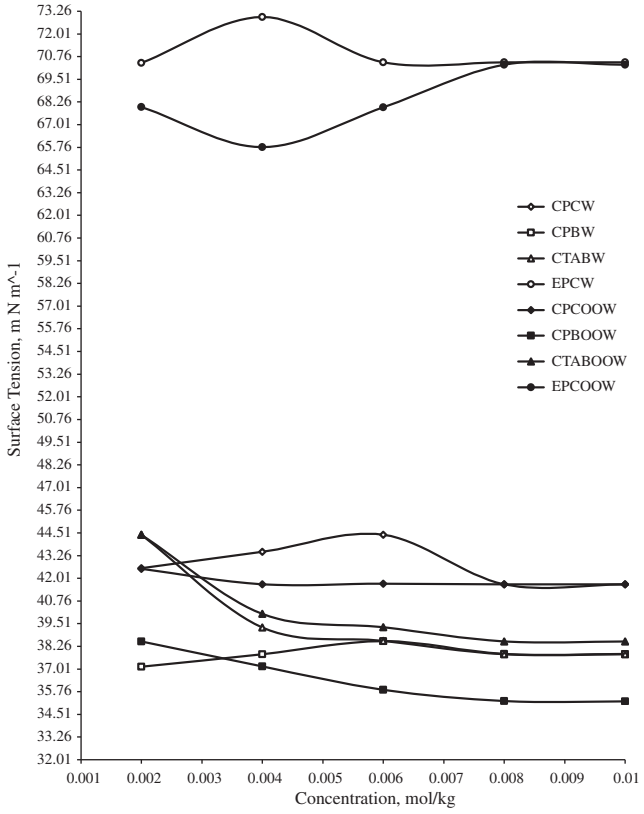

Figure 3 Surface tension (γ)/mN m^{-1} of the CPC, CPB, CTAB, and EPC systems.

but the head caused hydrophilic which reduces the surface tensions by more than 43% as compared to the EPC. The higher values of the CTAB are due to an effective reorientation caused by alkyl chain and N^+ ion and the higher IMF exerted by CTAB–OOW interactions. The EPC was not as effective as others with weaker disruption of water structure due to exertion of weaker IMMF and the EPC produced the lowest ρ^0 values. The EPC is a mild structure breaker with weaker IMF due to comparatively larger hydrophobic interaction developing units (HIDU). The EPC behaved as an excellent emulsifier only because of many forces centers are operational in developing interactions at separate points within a molecule. Hence it could not pushed to interface but remained suspended in hydrophilic water while the CPC, CPB, and CTAB reduced almost 43% ST as they tend to surface and saturate the same by reducing surface energy or tension due to integrated hydrophobic CBF but the EPC does not have integrated CBF along the alkyl chain because of the O atoms are in chains. Hence comparatively the EPC behaves as the best emulsifier while the CPC, CPB, and CTAB as the best cationic surfactants. This observation is also supported by an SEM pattern, with stronger intermolecular forces with CTAB and olive oil which produced a higher compatibility and density (Fig. 5).

A decrease in ρ^0 data of the CPC and EPC with olive oil–water from 0.99190 to 0.99150×10^3 kg m^{-3} is attributed to a swelling effect similar to sol gel formation with weaker internal forces (Fig. 1). The pyridine ring and the Cl^- ion of the CPC caused stronger hydrophilic interaction while the PO_4^{-3} of the EPC induced weaker forces. The EPC as BS showed a weaker ability to disrupt the water structure in comparison to others due to an emulsion formation with weaker cohesivity and densities. The slopes values with EPC are lower than of those of the others and inferred emulsification or homogenous dispersion in bulk water phase and not at surface contrary to CTAB, CPC, and CPB due to surface accumulation. Since with concentration the CTAB, CPC, and CPB move to surface and strongly weaken tension. Thus the slope values with composition are higher than those of the EPC where the IMMFT explained a maximum dissolution of the EPC. Thus the EPC is a suitable medium for transportation of bio-molecules with a weaker friction. The S_d values are as CPB > CPC > CTAB > EPC with the olive oil–water (Table 2). The CPB showed higher IMF with higher values while the PO_4^{-3} group with quaternary ammonium ion showed the lowest S_d values due to its effect on pair wise interactions. The CPB and CPC with olive oil–water forces exerted comparatively higher activity (Fig. 1).

3.2. Viscosities

The viscosity of water as a function intermolecular force is lower than of the BS–olive oil–water due to stronger Newtonian forces with water–BS interactions due to a destabilization of water structure. The CPC, CPB, and CTAB produced higher viscosities by 1.1 kg m^{-1} s^{-1} and the EPC had the 0.2 kg m^{-1} s^{-1} times than of the water which ensured their stronger water structure breaking effects (Table 1). The $(\eta_{rel} - 1)/c$ vs c analysis was polynomial (Eq. (3)) with positive B values (Table 2) as EPC > CPB > CPC > CTAB with 110.01,

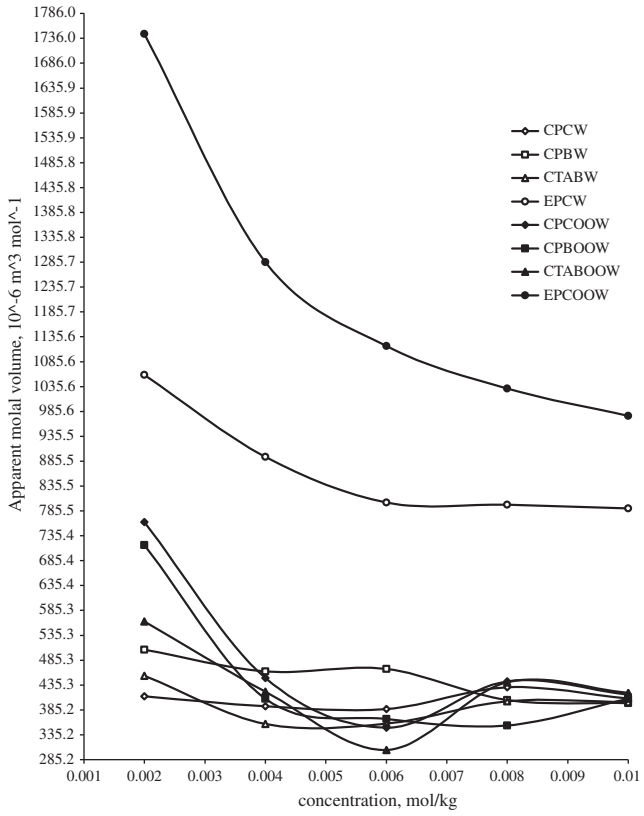

Figure 4 Apparent molal volume $(V_\phi)/10^{-6}\,m^3\,mol^{-1}$ with a sharp decrease from 0.002 to 0.01 mol kg^{-1} with distinct behavior of egg-phosphatidylcholine (EPC).

38.72, 37.55, and 37.21 kg mol^{-1}, respectively. The highest values of EPC with olive oil–water inferred comparatively stronger hydrophobic–hydrophobic interactions along emulsification supported with SEM analysis (Fig. 5). The EPC showed a stronger dispersion network with stronger solute–solute interactions while the CTAB as along dispersions and disrupted molecular surface. The molecular binding with EPC was less endothermic (Table 2) but increased with increments in alkyl-chain length and used its internal disorders as a driving force for binding. Thus the higher EPC viscosities inferred it as comparatively stronger water structure breaker. The ρ and V_ϕ data resolved Newtonian flow with lower water density than of the mixtures (Table 1) and dipolar interactions of BS are responsible for disrupting water structures. The stronger structural interactions occurred due to partially charged centers with higher values than the water. Resultants water monomers enter multiple force centers due to induction in alkyl chains and positively charged quaternary nitrogen atoms. The B coefficient is as CPC > CTAB > CPB > EPC inferred slightly weaker hydrophilic interactions with OOW over the hydrophobic. (Table 2).

3.3. Surface tension

The surface tensions of BS–olive oil–water are lower than of the water by 1.5 mN m^{-1} except the EPC, with slightly lower values (Table 1). With OOW, the higher surface forces than of the water are attributed to the stronger hydration spheres with the CPC, CPB, and CTAB. The γ^0 are as EPC > CTAB > CPC > CPB (Table 1) and are different than those of the ρ^0 and η^0 trends. The γ^0 data inferred a role of cohesive and adhesive forces due to activities in addition to electrostatic and Newtonian forces (Table 3).

A stronger ionic effect of a large sized Br^- anion enhanced hydrophobic–hydrophilic interactions between the CPB and OOW and produced a lowest γ^0 value with CPB. The CPB and CPC reoriented the water structures, with weaker surface forces due to a pyridine ring while the CTAB without π-conjugation did not show similar mechanism (Fig. 6). The higher γ^0 value with the EPC exerted a stronger IMF with stronger hydrophobic–hydrophobic interactions of longer alkyl chain. The IMMFT model explained an action mechanism of the EPC due to multiple force centers such as two alkyl chain, oxygen atoms, PO_4^{-3} group, and quaternary nitrogen atoms. The PO_4^{-3} group weakly disrupted the water, and highly asymmetricity in the EPC structure initiated the stronger cohesive forces. The higher entropic changes due to multiple force centers for interactions caused stronger hydrophobic–hydrophobic interactions (Singh and Matsuoka, 2009). The IMMFT predicted that the EPC molecules are not able to disrupt the hydrogen bonded water and the multiple forces of electrostatical points EPC exert higher tension. With such mixtures the hydrophobic interactions dominate by further attracting surface forces downwards with composition of the EPC. For example, from 8 mm kg^{-1} BS, the γ^0 values became linear with no further change in surface forces, due to a complete kind of the reorientation of water along little monomer formation (Fig. 3) which further increased with increasing concentration. The 8 mm kg^{-1} BS, initiated micelles formation, and is a critical micelle concentration point (Fig. 3). The S_γ values are negative, due to weaker cohesive forces with increase in compositions (Table 2). The SEM illustrated dispersed structures of biosurfactants with higher intermolecular forces between them in aqueous olive oil mixtures (Fig. 5). The IMMFT model excellently explained geometry of microstructures as a function of frictional and cohesive forces at multiple points, especially with the EPC. The molecular dispersion has maximum surface forces but an olive oil brought them together causing intermolecular forces which reduced an exposed area with reduction surface tension as EPC > CTAB > CPC > CPB. Their comparative study illustrated higher surface tension and lowest dispersion with EPC (Fig. 5). The stronger intermolecular forces between the EPC and EPC with higher cohesive and adhesive forces in olive oil–water are responsible for such a behavior. The SEM illustrated comparatively uniform dispersion with the EPC with weaker Van der Waals and London dispersion forces and is attributed to IMMFT.

3.4. Apparent molal volume

Apparent molal volume explained solute–solvent interactions with increments in concentrations. The molal volumes depicted an exertion of internal pressure caused by intermolecular forces where weaker are the forces higher are the volumes. The V_ϕ^0 data are EPC > CPC > CPB > CTAB with 1808.9 > 1078.2 > 983.7 > $751.4 \times 10^{-6}\,m^3 mol^{-1}$, respectively (Table 3), inferred weaker IMF with EPC + OOW. Of course, molecular size of the EPC is larger still higher volume showed weaker IMF. Positive V_ϕ^0 values inferred weaker internal pressure caused by weaker heteromolecular interactions. It is also true

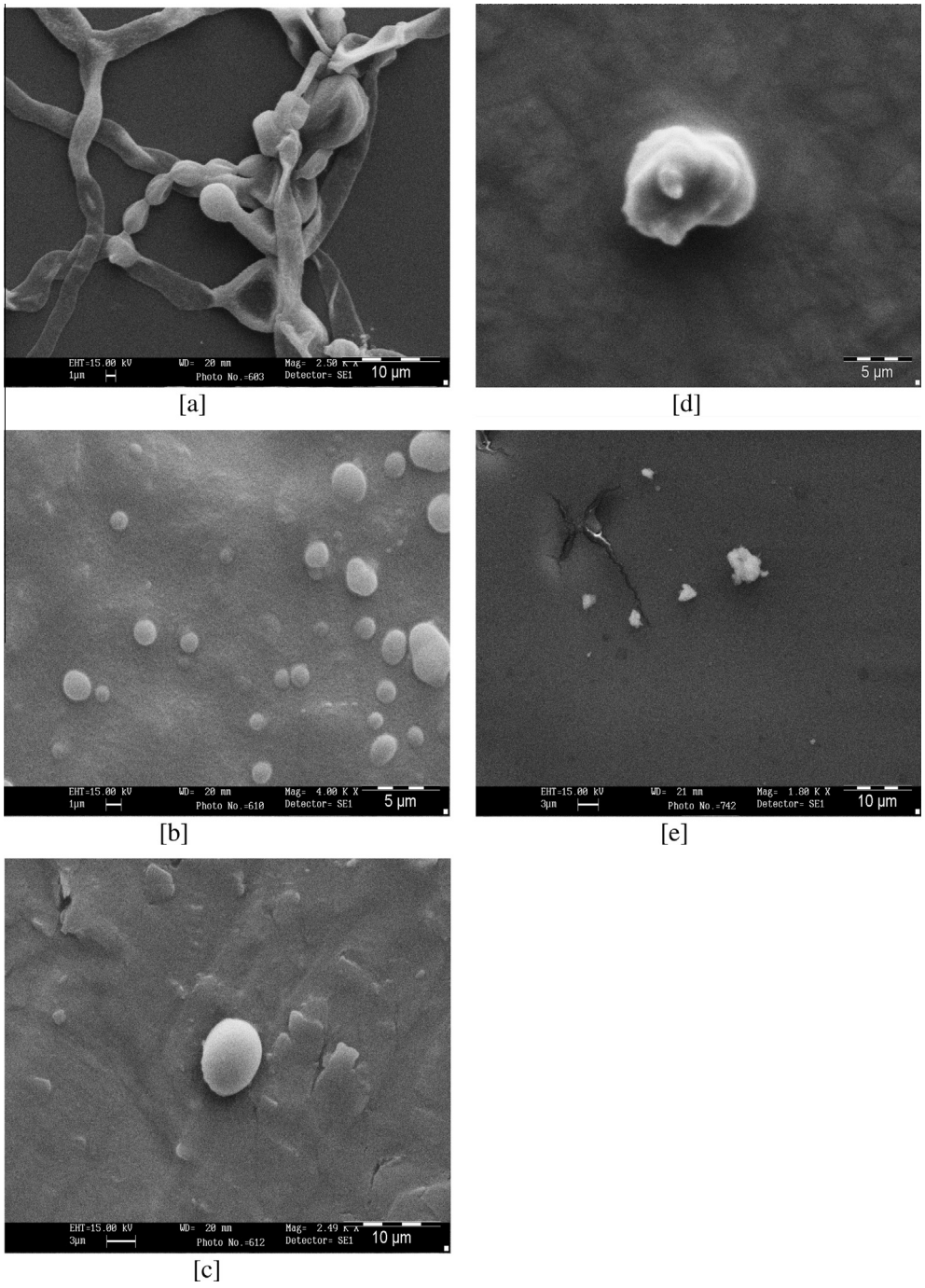

Figure 5 (a) The SEM of the olive oil in water (1:1000), (b) 0.1 M CPC with OOW, (c) 0.1 M CPB with OOW, (d) 0.1 M CTAB with OOW, and (e) 0.1 M EPC with OOW mixture.

in cases of the ρ^0 and η^0, the V_ϕ data with similar trends as transport and static properties respectively, with exceptional behavior of phosphate of the EPC. The V_ϕ values of the EPC decreased from 17450.0 to 976.8×10^{-6} m^3 mol^{-1} from 2 to 10 mm kg^{-1} with OOW, while the V_ϕ of the CPC, CPB, and CTAB decreased from 2 to 6 mm kg^{-1} but increased from 6 onwards (Fig. 4). It suspected micelles formation and surface saturation with CPC, CPB, and CTAB with two behaviors with lower and higher compositions while EPC did not show such a dual behavior with compositions which is explained due to IMMFT. As the multiple force centers inhibit surface saturation with EPC. In dilute concentration region, the interactions are weaker than those of the comparatively concentrated regions. The S_v and S'_v data inferred stronger solute–solute interactions of EPC than that of CPC, CPB, and CTAB (Table 3), with a crucial role of activation energy of phosphate–water interactions. The PO_4^{-3} caused an asymmetry in the EPC molecules with a maximum optimization as per a flickering model, the water molecules surround and adhered to the PO_4^{-3} with a stable conformation (Table 1).

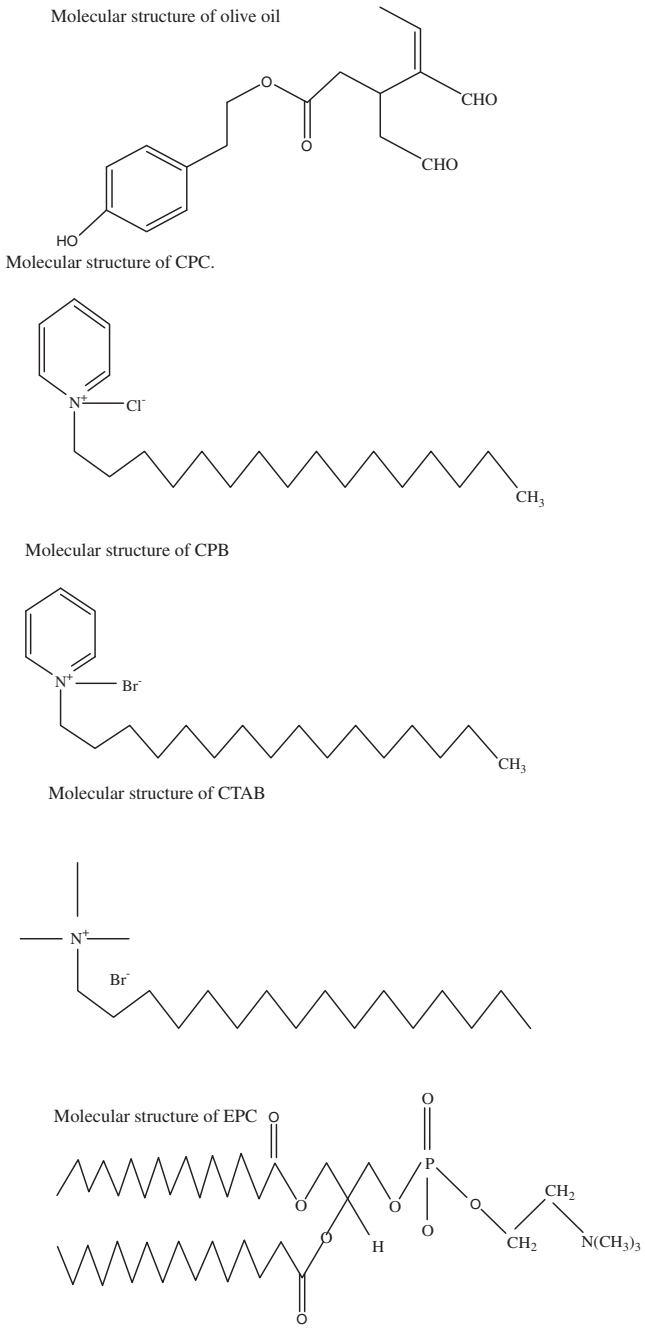

Figure 6 Molecular structure of olive oil, CPC, CPB, CTAB, and EPC.

3.5. SEM

With SEM, primary electrons are thermionically or field emitted by a cathode filament (W or LaB_6) or a field emission gun (W-tip) gets accelerated with high energy 1–30 KeV. The electron beam is steered with scanning coils over an area of interest, upon interaction with material, the primary electrons decelerated by transferring energy inelastically to other atomic electron and to the lattice of the sample. Due to continuous scattering events, the emitted radiation from the specimen are collected and used for imaging a topography of surface while characteristic X-rays emitted from the sample are analyzed to get information (quantitative and qualitative) about the elements present in the sample. Usually oil develops colloidal solution with diffuse interface forces while smaller biosurfactants are well defined hydrated units depicted by SEM. The biosurfactants breakdown the water structure while olive oil is not able to do so but it shifts the bulk structure of water around itself with a cage formation. The dispersion of the olive oil in water and of CPC, CPB, CTAB, and EPC molecules with olive oil–water mixture is depicted by the SEM as CTAB > CPC > CPB > EPC > OOW (Fig. 5). Here, the SEM studies illustrate that the olive oil structure in water does not get disrupted due to stronger intermolecular forces but it remains in its original structure. The thread like structure inferred the C backbone of olive oil (Fig. 5). The EPC has caused least disruption into *n*-fragmentations due to stronger solute–solute interactions, resulting with higher surface forces (Fig. 5). The CTAB though weakened the frictional forces but also caused some integrated or packed patches or the smaller globules which is dewetting (Fig. 5).

The CPC disrupted the structure of a surface alike the CPC molecule in clusters by weakening the cohesive forces (Fig. 5). The CPB further weakened IMF and strongly disrupted even clusters of olive oil, may be in a form of monomolecular layer and results into an effective structural reorientation (Fig. 5). The micrographs are of same concentration (0.1 m) varying their size from 5 to 10 μm in aqueous olive oil mixture (Fig. 5). The biosurfactants showed higher IMF in aqueous olive oil mixture due to stronger solute–solute and weaker solute–solvent interactions. The surfactants are highly soluble in

Table 3 Rates of viscosity and surface tension change with compositions which depict electrostatic or frictional and cohesive forces, respectively.

Concentration	Rate of viscosity change	Rate of surface tension change
	$\Delta\eta/\Delta c$	$\Delta\gamma/\Delta c$
CPC + OOW		
0.002	1.230	−425
0.004	3.180	5
0.006	0.135	−15
0.008	−0.470	5
0.010		
CPB + OOW		
0.002	0.735	−690
0.004	−0.755	−645
0.006	2.060	−310
0.008	1.795	−5
0.010		
CTAB + OOW		
0.002	1.110	−2170
0.004	0.965	−375
0.006	−1.205	−390
0.008	0.495	0.0
0.010		
EPC + OOW		
0.002	16.250	−1105
0.004	23.700	1095
0.006	16.700	1175
0.008	50.560	0.0
0.010		

water with stronger hydrogen bonding in water. Hence a molecular structure of the surface gets dispersed with weakening in cohesive and adhesive forces with olive oil–water mixture. The SEM depicted that the biosurfactants formed an integrated molecular solution due to hydrated hydrophilic forces with water while with olive oil get scattered due to the rising hydrophobic forces.

4. Biological significance

The IMMFT inferred a development of polarizable force fields which depends on the model used depicted by several workers such as Van der Waals and McLachlan. The McLachlan theory predicts that Van der Waals attractions in media are weaker than in vacuum based on like dissolves like where the different types of atoms interact more weakly than identical types of atoms. In contrast to combinatorial rules or Slater–Kirkwood model that illustrated classical force fields which were supported by Jacob Israelachvili with Intermolecular and surface forces model. The IMMFT model is advantageous by incorporating distribution of forces intramolecularly. It is refined model to avoid a central embarrassment of molecular mechanics like energy minimization or molecular dynamics. Our model of multiple force fields could be used for unfolding of protein structures for example, energies of hydrogen bonds in protein engineering. The IMMFT could clearly elucidate Lennard-Jones potentials in typical force fields in classes of organic compounds. The molecular biotics, fashionable configurations of atoms within spatial framework of covalent bonds, for example proteins, amino acid with intradisciplinary molecular structures like organic, semi-organic, complex, supramolecular prototypes activated chip. These perform several functions where Schrödinger quantum mechanics and wave mechanism of energy distribution and depictation occur. The theology of scientific up gradations on ionic to molecular coordination has now at center stage not because of nanotechnology but because of molecular potential to resolve various complicated issues of the matters. In this context, the IMMFT model is most suitable and a step forwards for resolving better understanding of the giants and supamolecular structures.

5. Conclusion

An interesting correlation between the physicochemical properties and the SEM microstructures was noted especially in case of the EPC which is a very common ingredient of the food digestion process. A fundamental difference in interacting behaviors in EPC and other surfactants CPC, CPB, and CTAB is of surface activities. With EPC due to IMMFT the EPC does not push to surface and could not reduce surface tension as compared to others which reduce about 43%. Since they saturate the surface due to stronger CBF but EPC is missing CBF. So EPC is a best emulsifier while the CPC, CVPB, and CTAB are best surfactants. With EPC three alkyl chains surround phosphate with steric and induction effects due to CBF and each alkyl has double bond with sp^2 configuration, also contribute to emulsification with negligible surface excess concentration. Hence IMMFT is an excellent model to structurally explain molecular forces responsible for emulsification action of the EPC as it has not largely reduced surface tension by not ending toward interface. Contrary to EPC, the CPC, CPB, and CTAB reduced surface tension more than 43% with higher surface excess concentration and comparatively stronger hydrophobic interaction than those of the hydrophilic.

The EPC is as excellent emulsifier only because of the many forces centers operation in developing interactions within single EPC molecule and is not pushed to interface but remained suspended in hydrophilic. Hence comparatively the EPC behaves as the best emulsifier, while the others as best cationic surfactants. The slopes values with EPC are lower than those of CPC, CPB, and CTAB because the EPC is emulsified or dispersed homogenously in bulk water phase. So the EPC does not move toward surface with increment in its concentration contrary to CTAB, CPC, and CPB which tend toward surface and get accumulated there on that seriously affect the surface tension. Higher concentration accumulation on surface needs higher work to be done and hence it strongly weakens tension. Thus the slopes with CPC, CPB, and CTAB concentrations the higher reduction in surface tension is required as compared to the EPC. Hence the IMMFT explained the maximum dissolution with EPC.

Acknowledgment

The authors are thankful to Principal, Deshbandhu College, University of Delhi, New Delhi, for infrastructural support.

References

Brunger, A.T., Adams, P.D., 2002. Molecular dynamics applied to X-ray structure refinement. Acc. Chem. Res. 35, 404–412.
Edgcomb, S.P., Murphy, K.P., 2001. Structural energetics of protein folding and binding. Curr. Opin. Biotechnol. 11, 62–66.
Graziano, G., Catanzano, F., Del Vecchio, P., Giancola, C., Barone, G., 1996. Thermodynamic stability of globular proteins: a reliable model from small molecule studies. Gazetta Chim. Italiana 126, 559–567.
Guntert, P., 1998. Structure calculation of biological macromolecules from NMR data. Q. Rev. Biophys. 31, 145–237.
Israelachvili, J.N., 1992. Intermolecular and Surface Forces. Academic Press, San Diego.
Koehl, P., Levitt, M., 1999. A brighter future for protein structure prediction. Nat. Struct. Biol. 6, 108–111.
Leckband, D., Israelachvili, J., 2001. Intermolecular forces in biology. Q. Rev. Biophys. 34, 105–267.
Lomize, A.L., Reibarkh, M.Y., Pogozheva, I.D., 2002. Interatomic potentials and solvation parameters from protein engineering data for buried residues. Protein Sci. 11, 1984–2000.
Lomize, A.L., Pogozheva, I.D., Lomize, M.A., Mosberg, H.I., 2006. Positioning of proteins in membranes: a computational approach. Protein Sci. 15, 1318–1333.
Mendes, J., Guerois, R., Serrano, L., 2002. Energy estimation in protein design. Curr. Opin. Struct. Biol. 12, 441–446.
Murphy, K.P., Gill, S.J., 1991. Solid model compounds and the thermodynamics of protein unfolding. J. Mol. Biol. 222, 699–709.
Myers, J.K., Pace, C.N., 1996. Hydrogen bonding stabilizes globular proteins. Biophys. J. 71, 2033–2039.
Ponder, J.W., Case, D.A., 2003. Force fields for protein simulations. Adv. Protein Chem. 66, 27–85.
Rohl, C.A., Strauss, C.E.M., Misura, K.M.S., Baker, D., 2004. Protein structure prediction using Rosetta. Methods Enzymol. 383, 66–93.
Schutz, C.N., Warshel, A., 2001. What are the dielectric "constants" of proteins and how to validate electrostatic models? Proteins 44, 400–417.

Shakhnovich, E.I., Finkelstein, A.V., 1989. Theory of cooperative transitions in protein molecules. I. Why denaturation of globular proteins is a first-order phase transition. Biopolymers 28, 1667–1680.

Singh, M., 2006. Survismeter-type 1 and 2 for surface tension and viscosity measurements of liquids for academic, and research and development studies. J. Biochem. Biophys. Methods 67 (2–3), 151–161.

Singh, M., 2009. Cutting edge device over usual surface tension, interfacial tension, viscosity, experimental measurements for saturated hydrocarbons and dithioerythritol: air filter fitted survismeter. Bulg. J. Chem. Edu. 18 (5), 159–164.

Singh, M., Kumar, A., 2006. Hydrophobic interactions of *N*-methylureas in aqueous solutions estimation from density, molal volume, viscosity and surface tension. J. Sol. Chem. 35 (4), 582–587.

Singh, M., Matsuoka, H., 2009. Liquid–liquid interface study of hydrocarbons, alcohols and cationic surfactants with water. Surf. Rev. Lett. 16 (4), 509–608.

Singh, M., Sharma, Y.K., 2006. Phys. Chem. Liq. 44, 1–14.

Singh, M., Sushma, 2009. Studies of densities, apparent molal volume, viscosities, surface tension and free energies of activation for interactions of Praseodymium Sal_2en complex with dimethylsulphoxide. J. Mol. Liq. 148, 6–12.

Singh, M., Yadav, D., Yadav, R.K., 2008. Preparation, structural elucidation, molecular weight determination, and molecular recognition of first- and second-tier dendrimer molecules. J. Appl. Polym. Sci. 110 (5), 2601–2614.

Warshel, A., Levitt, M., 1976. Theoretical studies of enzymatic reactions: dielectric electrostatic and steric stabilization of the carbonium ion in the reaction of lysozyme. J. Mol. Biol. 103, 227–249.

Warshel, A., Sharma, P.K., Kato, M., Parson, W.W., 2006. Modeling electrostatic effects in proteins. Biochim. Biophys. Acta 1764, 1647–1676.